

# INCORPORATING CORRELATIONS BETWEEN DRUGS AND HETEROGENEITY OF MULTI-OMICS DATA IN STRUCTURED PENALIZED REGRESSION FOR DRUG SENSITIVITY PREDICTION

BY ZHI ZHAO AND MANUELA ZUCKNICK

*Department of Biostatistics, University of Oslo  
P.O.Box 1122 Blindern 0317 Oslo, Norway*

Targeted cancer drugs have been developed to interfere with specific molecular targets, which are expected to affect the growth of cancer cells in a way that can be characterized by multi-omics data. The prediction of cancer drug sensitivity simultaneously for multiple drugs based on heterogeneous multi-omics data (e.g., mRNA expression, DNA copy number or DNA mutation) is an important but challenging task. We use joint penalized regression models for multiple cancer drugs rather than a separate model for each drug, thus being able to address the correlation structure between drugs. In addition, we employ integrative penalty factors (IPF) to allow penalizing data from different molecular data sources differently. By integrating IPF with tree-lasso, we create the IPF-tree-lasso method, which can capture the heterogeneity of multi-omics data and the correlation between drugs at the same time. Additionally, we generalize the IPF-lasso to the IPF-elastic-net, which combines  $\ell_1$ - and  $\ell_2$ -penalty terms and can lead to improved prediction performance. To make the computation of IPF-type methods more feasible, we present that the IPF-type methods are equivalent to the original lasso-type methods after augmenting the data matrix, and employ the Efficient Parameter Selection via Global Optimization (EPSGO) algorithm for optimizing multiple penalty factors efficiently. Simulation studies show that the new model, IPF-tree-lasso, can improve the prediction performance significantly. We demonstrate the performance of these methods on the Genomics of Drug Sensitivity in Cancer (GDSC) data.

**1. Introduction.** Many cancers have specific molecular causes, e.g., mutations in genes involved in the hallmark processes of cancer [16]. Targeted cancer drugs directly affect those particular cancer genes. However, the efficacy of a drug to block cancer cells' growth may be determined by additional genes. For example, trastuzumab is a human epidermal growth factor receptor-2 (HER2) antibody targeting HER2-overexpressed breast cancer cells [8]. But Liu *et al.* [28] reported that  $\beta_2$ -adrenergic receptor

---

*Keywords and phrases:* Genomics of Drug Sensitivity in Cancer (GDSC), Integrative penalty factors, Multivariate penalized regression, Structured penalty, Tree-lasso

( $\beta$ 2-AR) is also a molecular marker to affect the efficacy of trastuzumab in breast cancer. The other example is that the drug Vemurafenib targets metastatic melanoma BRAF mutations at codon 600 [29]. But the matrix metalloproteinase-2 (MMP-2) upregulation has been found in vemurafenib-resistant melanoma cells [34]. Therefore, exploring the multi-omics data which can characterize the whole biological system is helpful to evaluate drug efficacy. It is also potential to find new cancer therapy solutions. That is, cancer cells with the similar characterization of multi-omics are possibly affected by other drugs. Thus it is valuable to model multiple cancer drugs sensitivity and multi-omics data jointly.

In recent years, several groups and consortia have developed big datasets which include large-scale ex vivo pharmacological profiling of cancer drugs and the genomic information of corresponding cell lines [3, 9, 13, 15, 18]. The genomic data can for example consist of genome-wide measurements of mRNA expression, DNA copy numbers, DNA single-point and other mutations or CpG methylation of cell lines. They reflect different heterogeneous molecular profiles of the cancer cell lines with respect to effects, intra correlations, measurement scales and background noise [17]. The drug sensitivity data for some groups of drugs are expected to be correlated, due to their common targets and similar pharmacodynamic behaviours.

To analyze such data, one straightforward method is to use (penalized) linear regression methods, for example lasso [42], regressing each drug on all molecular features in a linear manner. Lasso could select a few relevant features with nonzero regression coefficient estimates from a large number of features. But it cannot address the heterogeneity of different molecular data sources. Boulesteix *et al.* [5] introduced integrative  $\ell_1$ -penalized regression with penalty factors (IPF-lasso) to shrink the effects of features from different data sources with varying  $\ell_1$ -penalties, to reflect their different relative contributions. While lasso or IPF-lasso can be extended to multivariate regression to jointly model multiple drugs sensitivity, the correlation of drugs is not reflected in the penalization of regression coefficients. Kim and Xing [22] proposed tree-lasso to estimate structured sparsity of multiple response variables assuming a hierarchical cluster structure in the response variables. Each cluster is likely to be influenced by some common features, for which the effects are similar between correlated responses.

In this article, we propose the IPF-tree-lasso which borrows the strength of varying penalty parameters from IPF-lasso and the cluster structure in multivariate regression from tree-lasso. Thus, IPF-tree-lasso can capture the different relative contributions of multiple omics input data sources and the group structure of correlated drug response variables. Since some targeted

cancer drugs might have a similar mechanisms, for example the same target gene or signaling pathway, then these drugs are likely to have correlated sensitivities. IPF-tree-lasso is likely to select common relevant molecular features of these correlated drugs, and accordingly to shrink their coefficients with similar penalty parameters.

Elastic net [50] is also compared here, because it considers the grouping effect of correlated features and the  $\ell_2$ -penalty can improve the prediction performance over lasso. Additionally, we also formulate the integrative elastic net with penalty factors (IPF-elastic-net) model to provide a flexible extension of the elastic net with varying complexity parameters  $\lambda$ 's as well as varying parameters  $\alpha$ 's.

However, IPF-tree-lasso and IPF-elastic-net have more complicated penalty terms which might require new optimization algorithms. We use augmented data matrix, so that the original smoothing proximal gradient descent method [22] and cyclical coordinate descent algorithm for lasso [11] can be employed directly. As elastic net and IPF-type methods have multiple penalty parameters to be optimized, the standard grid search [21] is computationally not efficient. Frohlich and Zell [12] proposed an interval-search algorithm, the Efficient Parameter Selection via Global Optimization (EPSGO), which is more efficient. Sill *et al.* [37] implemented the EPSGO algorithm in elastic net models and developed the R package `c060`. We have adapted the `c060` package for efficient penalty parameters optimization for IPF-tree-lasso and IPF-elastic-net.

The rest of the paper is organized as follows. In Section 2, the standard penalized regression methods and their extensions with structured penalties are introduced briefly. Section 3 describes the simulation scenario based on multivariate responses and different types of features, and then we present the simulation results and discussion. In Section 4, the Genomics of Drug Sensitivity in Cancer [13] data are used to compare the prediction performance of all methods. Lastly, we discuss the main findings and conclude the paper in Section 5.

## 2. Structured penalties for multivariate regression.

2.1. *Lasso and elastic net.* The pharmacological data are collected for  $n$  samples (e.g., cell lines or patients) and  $m$  response variables (typically drug sensitivity). The response variables are denoted by  $\mathbf{Y} = \{y_{ik}\}$  ( $i \in [n] \equiv \{1, \dots, n\}$ ,  $k \in [m]$ ), where  $y_{ik}$  means the response of the  $i$ th cell line treated with the  $k$ th drug. The high-dimensional (i.e., multi-omics) data contain  $p$  features in total, and all  $p$  features are available for all samples, denoted by  $\mathbf{X} = \{x_{ij}\}$  ( $i \in [n]$ ,  $j \in [p]$ ). The linear model mapping from

high-dimensional data to multivariate responses is

$$(2.1) \quad \mathbf{Y} = \mathbf{1}_n \boldsymbol{\beta}_0^\top + \mathbf{X}\mathbf{B} + \mathbf{E},$$

where  $\mathbf{1}_n = (1, \dots, 1)^\top$  is an  $n$ -column vector,  $\boldsymbol{\beta}_0 = (\beta_{01}, \dots, \beta_{0m})^\top$  is the intercept vector corresponding to  $m$  response variables,  $\mathbf{B}$  is a  $p \times m$  regression coefficients matrix, and  $\mathbf{E}$  is a  $n \times m$  noise matrix.  $(\boldsymbol{\beta}_0, \mathbf{B})$  can be estimated by minimizing the sum of the residual sum of squares and a penalty function as following

$$(2.2) \quad \min_{\boldsymbol{\beta}_0, \mathbf{B}} \left\{ \frac{1}{2mn} \|\mathbf{Y} - \mathbf{1}_n \boldsymbol{\beta}_0^\top - \mathbf{X}\mathbf{B}\|_F^2 + \text{pen}(\mathbf{B}) \right\},$$

where  $\|\cdot\|_F$  is the Frobenius norm. When  $p$  is very large, especially  $n \ll p$ , and presuming only a few true relevant features, the  $\ell_1$ -penalized regression, or lasso [42] is a standard method to identify those features by their nonzero coefficient estimates. The multivariate lasso uses the  $\ell_1$ -norm penalty function  $\text{pen}(\mathbf{B}) = \lambda \|\mathbf{B}\|_{\ell_1}$  in (2.2), where  $\|\mathbf{B}\|_{\ell_q} = (\sum_{j,k} |\beta_{jk}|^q)^{1/q}$  ( $q \in [1, \infty)$ ) and  $\lambda > 0$  is the given penalty parameter that controls the strength of penalizing coefficients.

Another regularization method is elastic net [50], which takes a bias-variance trade-off between lasso and the continuous shrinkage method ridge regression. The ridge penalty ( $\ell_2$ -penalty) tends to include or exclude strongly correlated features together. The penalty function of elastic net in (2.2) is  $\text{pen}(\mathbf{B}) = \lambda(\alpha \|\mathbf{B}\|_{\ell_1} + \frac{1}{2}(1-\alpha) \|\mathbf{B}\|_{\ell_2}^2)$ , where  $\alpha \in [0, 1]$  gives the compromise between ridge ( $\alpha = 0$ ) and lasso ( $\alpha = 1$ ).

## 2.2 IPF-lasso and IPF-elastic-net

Lasso and elastic net penalize all coefficients of features by globally controlling penalty parameters  $\lambda$  and  $\alpha$ . In order to distinguish the contributions of heterogeneous data sources, Boulesteix *et al.* [5] proposed IPF-lasso to analyze multi-omics data. IPF-lasso allows varying penalty parameters to weight the norms of different sources' coefficients. For multivariate responses, the penalty function is  $\text{pen}(\mathbf{B}) = \sum_s \lambda_s \|\mathbf{B}_s\|_{\ell_1}$  ( $s \in [S]$ ), where  $\lambda_s > 0$ ,  $\mathbf{B} = [\mathbf{B}_1 \vdots \dots \vdots \mathbf{B}_S]$  stacks  $\mathbf{B}_s$  by rows and  $\mathbf{B}_s$  is the coefficients matrix corresponding to the  $s$ th data source. The IPF-lasso reduces to the lasso problem after transforming the  $\mathbf{X}$  matrix as follows.

**PROPOSITION 1.** *Given response  $\mathbf{Y}$  and  $S$  data sources  $\mathbf{X} = [\mathbf{X}_1, \dots, \mathbf{X}_S]$  with numbers of features  $p_1, \dots, p_S$  respectively, and the corresponding co-*

efficient matrix  $\mathbf{B} = [\mathbf{B}_1 : \dots : \mathbf{B}_S]$ , let

$$\begin{aligned}\mathbf{X}^* &= \left[ \mathbf{X}_1, \frac{\lambda_1}{\lambda_2} \mathbf{X}_2, \dots, \frac{\lambda_1}{\lambda_S} \mathbf{X}_S \right] \in \mathbb{R}^{n \times (p_1 + \dots + p_S)}, \\ \mathbf{B}^* &= \left[ \mathbf{B}_1 : \frac{\lambda_2}{\lambda_1} \mathbf{B}_2 : \dots : \frac{\lambda_S}{\lambda_1} \mathbf{B}_S \right] \in \mathbb{R}^{(p_1 + \dots + p_S) \times m}, \\ (\hat{\beta}_0, \hat{\mathbf{B}}) &= \arg \min_{\beta_0, \mathbf{B}} \left\{ \frac{1}{2mn} \|\mathbf{Y} - \mathbf{1}_n \beta_0^\top - \mathbf{X} \mathbf{B}\|_F^2 + \sum_{s=1}^S \lambda_s \|\mathbf{B}_s\|_{\ell_1} \right\}, \\ (\hat{\beta}_0, \hat{\mathbf{B}}^*) &= \arg \min_{\beta_0, \mathbf{B}^*} \left\{ \frac{1}{2mn} \|\mathbf{Y} - \mathbf{1}_n \beta_0^\top - \mathbf{X}^* \mathbf{B}^*\|_F^2 + \lambda_1 \|\mathbf{B}^*\|_{\ell_1} \right\}.\end{aligned}$$

Then  $\hat{\mathbf{B}}^* = \left[ \hat{\mathbf{B}}_1 : \frac{\lambda_2}{\lambda_1} \hat{\mathbf{B}}_2 : \dots : \frac{\lambda_S}{\lambda_1} \hat{\mathbf{B}}_S \right]$ , where  $\hat{\mathbf{B}} = [\hat{\mathbf{B}}_1 : \hat{\mathbf{B}}_2 : \dots : \hat{\mathbf{B}}_S]$ .

When there are two data sources, i.e.,  $S = 2$ , Figure 1 shows that the prediction performance as cross-validated  $\text{MSE}_{\text{CV}}$  is convex in versus  $\lambda_1$  when fixing the two penalty parameters ratio  $\lambda_2/\lambda_1$ .

A simple integrative  $\ell_1/\ell_2$ -penalty method with penalty factors (sIPF-elastic-net) has  $\text{pen}(\mathbf{B}) = \sum_s \lambda_s (\alpha \|\mathbf{B}_s\|_{\ell_1} + \frac{1}{2}(1 - \alpha) \|\mathbf{B}_s\|_{\ell_2}^2)$  where  $\lambda_s > 0$  ( $s \in [S]$ ) and  $\alpha \in [0, 1]$ . Here, different data sources share the same parameter  $\alpha$ , which forces the same strength to shrink the coefficients of strongly correlated features towards each other.

**THEOREM 1.** *Given  $n$  samples and  $m$  responses  $\mathbf{Y}$ , standardized  $S$  data sources  $\mathbf{X} = [\mathbf{X}_1, \dots, \mathbf{X}_S]$  (variance 1 and mean 0 for each column) with numbers of features  $p_1, \dots, p_S$ , respectively, and the corresponding coefficients matrix  $\mathbf{B}$ , let  $\boldsymbol{\lambda} = (\lambda_1, \dots, \lambda_S)$ , and  $\hat{\beta}_0(\boldsymbol{\lambda}, \alpha)$ ,  $\hat{\mathbf{B}}(\boldsymbol{\lambda}, \alpha)$  be the sIPF-elastic-net estimates. Suppose two coefficients  $\beta_{jk}$  and  $\beta_{j'k}$  from the  $s$ th and  $s'$ th data sources ( $j, j' \in [p], j \neq j'; s, s' \in [S]; k \in [m]$ ), respectively, and  $\hat{\beta}_{jk}(\boldsymbol{\lambda}, \alpha) \hat{\beta}_{j'k}(\boldsymbol{\lambda}, \alpha) > 0$ ; then*

$$|\hat{\beta}_{jk}(\boldsymbol{\lambda}, \alpha) - \hat{\beta}_{j'k}(\boldsymbol{\lambda}, \alpha)| \leq \frac{\sqrt{\lambda_s^2 + \lambda_{s'}^2 - 2\lambda_s \lambda_{s'} \rho}}{mn \lambda_s \lambda_{s'} (1 - \alpha)} \|\mathbf{Y}\|_{\ell_1},$$

where sample correlation  $\rho = \mathbf{x}_{s,j}^\top \mathbf{x}_{s',j'}$  with  $\mathbf{x}_{s,j}$  the vector of  $n$  samples of the  $j$ th feature belonging to the  $s$ th data source and  $\|\mathbf{Y}\|_{\ell_1} = \sum_{i=1}^n \sum_{k=1}^m |y_{ik}|$ .

Theorem 1 (proof in Supplementary S1) states that the difference of two nonzero and the same sign coefficient estimates tends to 0 if their corresponding features are highly positively correlated and penalized equally. Therefore, sIPF-elastic-net shows the similar grouping effect as elastic net. The

fully flexible version of the IPF-elastic-net has penalty function  $\text{pen}(\mathbf{B}) = \sum_s \lambda_s (\alpha_s \|\mathbf{B}_s\|_{\ell_1} + \frac{1}{2}(1 - \alpha_s) \|\mathbf{B}_s\|_{\ell_2}^2)$ , where  $\lambda_s > 0$ ,  $\alpha_s \in [0, 1]$  ( $s \in [S]$ ). Proposition 2 gives its equivalent lasso problem if  $\alpha_s \in (0, 1]$ .

**PROPOSITION 2.** *Given response  $\mathbf{Y}$  and  $S$  data sources  $\mathbf{X} = [\mathbf{X}_1, \dots, \mathbf{X}_S]$  with numbers of features  $p_1, \dots, p_S$  respectively, and the corresponding coefficients matrix is  $\mathbf{B} = [\mathbf{B}_1 : \dots : \mathbf{B}_S]$ , let*

$$(2.3) \quad \begin{aligned} (\hat{\beta}_0, \hat{\mathbf{B}}) &= \arg \min_{\beta_0, \mathbf{B}} \left\{ \frac{1}{2mn} \|\mathbf{Y} - \mathbf{1}_n \beta_0^\top - \mathbf{X} \mathbf{B}\|_F^2 + \sum_{s=1}^S \lambda_s (\alpha_s \|\mathbf{B}_s\|_{\ell_1} + \frac{1}{2}(1 - \alpha_s) \|\mathbf{B}_s\|_{\ell_2}^2) \right\}, \\ (\hat{\beta}_0, \hat{\mathbf{B}}^*) &= \arg \min_{\beta_0, \mathbf{B}^*} \left\{ \frac{1}{2mn} \|\mathbf{Y}^* - \mathbf{1}_{n+p} \beta_0^\top - \mathbf{X}^* \mathbf{B}^*\|_F^2 + \lambda_1^* \|\mathbf{B}^*\|_{\ell_1} \right\}. \end{aligned}$$

Then  $\hat{\mathbf{B}}^* = [\alpha_1 \hat{\mathbf{B}}_1 : \frac{\alpha_2 \lambda_2}{\lambda_1} \hat{\mathbf{B}}_2 : \dots : \frac{\alpha_S \lambda_S}{\lambda_1} \hat{\mathbf{B}}_S]$ , where

$$\mathbf{X}^* = \begin{bmatrix} \frac{1}{\alpha_1} \mathbf{X}_1 & \frac{\lambda_1}{\alpha_2 \lambda_2} \mathbf{X}_2 & \dots & \frac{\lambda_1}{\alpha_S \lambda_S} \mathbf{X}_S \\ \frac{1}{\alpha_1} \sqrt{\frac{1}{2} \lambda_1 (1 - \alpha_1)} \mathbb{I}_{p_1} & \mathbf{0} & \dots & \mathbf{0} \\ \mathbf{0} & \frac{\lambda_1}{\alpha_2 \lambda_2} \sqrt{\frac{1}{2} \lambda_2 (1 - \alpha_2)} \mathbb{I}_{p_2} & \dots & \mathbf{0} \\ \vdots & \vdots & \ddots & \vdots \\ \mathbf{0} & \mathbf{0} & \dots & \frac{\lambda_1}{\alpha_S \lambda_S} \sqrt{\frac{1}{2} \lambda_S (1 - \alpha_S)} \mathbb{I}_{p_S} \end{bmatrix} \in \mathbb{R}^{(n+p) \times p},$$

$$\mathbf{Y}^* = [\mathbf{Y} : \mathbf{0} : \dots : \mathbf{0}] \in \mathbb{R}^{(n+p) \times m},$$

$$\mathbf{B}^* = [\alpha_1 \mathbf{B}_1 : \frac{\alpha_2 \lambda_2}{\lambda_1} \mathbf{B}_2 : \dots : \frac{\alpha_S \lambda_S}{\lambda_1} \mathbf{B}_S] \in \mathbb{R}^{p \times m},$$

$$\lambda_1^* = \lambda_1 / \{2m(n + \sum_s p_s)\},$$

$$\alpha_s \in (0, 1], s \in 1, \dots, S.$$

**2.2. Tree-lasso and IPF-tree-lasso.** Kim and Xing [22] proposed the tree-lasso method which uses a hierarchical tree structure over the response variables in a group-lasso based penalty function. As illustrated in Figure 2 we hypothesize that highly correlated response variables in each cluster are likely to be influenced by a common set of features. The hierarchical tree structure of multiple response variables can be represented as a tree  $T$  with a set of vertices  $V$  and groups  $\{G_\nu : \nu \in V\}$ . It can be given by prior knowledge of the pharmacokinetic properties of the drugs, or be learned from the data, for example by hierarchical clustering. Given the tree  $T$  and groups

$G_\nu$ , the penalty function of the tree-lasso is defined as

$$\begin{aligned}
 \text{pen}(\mathbf{B}) &= \lambda \sum_{j=1}^p \sum_{\nu \in V} \omega_\nu \|\beta_j^{G_\nu}\|_{\ell_2} \\
 &= \lambda \sum_{j=1}^p \sum_{\nu \in V_{\text{leaf}}} \|\beta_j^{G_\nu}\|_{\ell_2} + \lambda \sum_{j=1}^p \sum_{\nu \in V_{\text{int}}} \omega_\nu \|\beta_j^{G_\nu}\|_{\ell_2} \\
 &= \lambda \sum_{j=1}^p \sum_{\nu \in V_{\text{leaf}}} |\beta_j^{G_\nu}| + \lambda \sum_{j=1}^p \sum_{\nu \in V_{\text{int}}} \{h_\nu \cdot \sum_{c \in \text{Children}(\nu)} \omega_c \|\beta_j^{G_c}\|_{\ell_2} + (1 - h_\nu) \|\beta_j^{G_\nu}\|_{\ell_2}\},
 \end{aligned}$$

where  $\beta_j^{G_\nu} = \{\beta_{jk} : k \in G_\nu\}$  is the  $j$ th row of  $\mathbf{B}$  associated with response variables in group  $\nu$ ,  $\omega_\nu$  is either the weight associated with the height  $h_\nu$  of each internal node in tree  $T$  or  $\omega_\nu = 1$  for the leaf node,  $V_{\text{int}}$  and  $V_{\text{leaf}}$  are the internal nodes and leaves of the tree, respectively. For example, consider a case with two drugs and a tree of three nodes that consists of two leaf nodes and one root node. It is illustrated as the following subtree of tree  $T$  in Figure 2,  $V = \{\nu_1, \nu_2, \nu_4\}$ ,  $\beta_j^{G_{\nu_1}} = \{\beta_{j1} : j \in [p]\}$ ,  $\beta_j^{G_{\nu_2}} = \{\beta_{j2} : j \in [p]\}$ ,  $\beta_j^{G_{\nu_4}} = \{\beta_{jk} : j \in [p]; k \in \{1, 2\}\}$ . Then the penalty function for this tree is (2.4)

$$\text{pen}(\mathbf{B}) = \lambda \sum_{j=1}^p \left\{ \underbrace{|\beta_{j1}|}_{\text{leaf } G_{\nu_1}} + \underbrace{|\beta_{j2}|}_{\text{leaf } G_{\nu_2}} + h_{\nu_4} \left( \underbrace{|\beta_{j1}|}_{\text{leaf } G_{\nu_1}} + \underbrace{|\beta_{j2}|}_{\text{leaf } G_{\nu_2}} \right) + (1 - h_{\nu_4}) \underbrace{\sqrt{(\beta_{j1})^2 + (\beta_{j2})^2}}_{\text{internal } G_{\nu_4}} \right\}.$$

We can now define IPF-tree-lasso, where different  $\lambda$ 's are employed for different data sources. Its penalty function is defined as follows

$$(2.5) \quad \text{pen}(\mathbf{B}) = \sum_{s=1}^S \lambda_s \left( \sum_{j=1}^{p_s} \sum_{\nu \in V_{\text{int}}} \omega_\nu \|\beta_{j,s}^{G_\nu}\|_{\ell_2} + \sum_{j=1}^{p_s} \sum_{\nu \in V_{\text{leaf}}} \|\beta_{j,s}^{G_\nu}\|_{\ell_2} \right),$$

where  $\beta_{j,s}$  is the  $j$ th row of coefficients corresponding to  $s$ th data source.

**PROPOSITION 3.** *Given response  $\mathbf{Y}$  and  $S$  data sources  $\mathbf{X} = [\mathbf{X}_1, \dots, \mathbf{X}_S]$  with numbers of features  $p_1, \dots, p_S$ , respectively, and the corresponding co-*

efficient matrix is  $\mathbf{B} = [\mathbf{B}_1 : \dots : \mathbf{B}_S]$ , let

$$\mathbf{X}^* = \left[ \mathbf{X}_1, \frac{\lambda_1}{\lambda_2} \mathbf{X}_2, \dots, \frac{\lambda_1}{\lambda_S} \mathbf{X}_S \right] \in \mathbb{R}^{n \times (p_1 + \dots + p_S)},$$

$$\mathbf{B}^* = \left[ \mathbf{B}_1 : \frac{\lambda_2}{\lambda_1} \mathbf{B}_2 : \dots : \frac{\lambda_S}{\lambda_1} \mathbf{B}_S \right] \in \mathbb{R}^{(p_1 + \dots + p_S) \times n},$$

$$(\hat{\boldsymbol{\beta}}_0, \hat{\mathbf{B}}) = \arg \min_{\boldsymbol{\beta}_0, \mathbf{B}} \left\{ \frac{1}{2mn} \|\mathbf{Y} - \mathbf{1}_n \boldsymbol{\beta}_0^\top - \mathbf{X} \mathbf{B}\|_F^2 + \sum_{s=1}^S \lambda_s \left( \sum_{j=1}^{p_s} \sum_{\nu \in V_{int}} \omega_\nu \|\boldsymbol{\beta}_{j,s}^{G_\nu}\|_{\ell_2} + \sum_{j=1}^{p_s} \sum_{\nu \in V_{leaf}} \|\boldsymbol{\beta}_{j,s}^{G_\nu}\|_{\ell_2} \right) \right\}$$

$$(\hat{\boldsymbol{\beta}}_0, \hat{\mathbf{B}}^*) = \arg \min_{\boldsymbol{\beta}_0, \mathbf{B}^*} \left\{ \frac{1}{2mn} \|\mathbf{Y} - \mathbf{1}_n \boldsymbol{\beta}_0^\top - \mathbf{X}^* \mathbf{B}^*\|_F^2 + \lambda_1 \left( \sum_j^p \sum_{\nu \in V_{int}} \omega_\nu \|\boldsymbol{\beta}_j^{*G_\nu}\|_{\ell_2} + \sum_j^p \sum_{\nu \in V_{leaf}} \|\boldsymbol{\beta}_j^{*G_\nu}\|_{\ell_2} \right) \right\}$$

Then  $\hat{\mathbf{B}}^* = \left[ \hat{\mathbf{B}}_1 : \frac{\lambda_2}{\lambda_1} \hat{\mathbf{B}}_2 : \dots : \frac{\lambda_S}{\lambda_1} \hat{\mathbf{B}}_S \right]$ , where  $\hat{\mathbf{B}} = [\hat{\mathbf{B}}_1 : \hat{\mathbf{B}}_2 : \dots : \hat{\mathbf{B}}_S]$ .

Without loss of generality, the proof for the case with three response variables and the tree of five nodes shown in Figure 2 is given in Supplementary S2.

PROPOSITION 4. *Generally, the penalized objective function can be formulated as*

$$(2.6) \quad \min_{\boldsymbol{\beta}_0, \mathbf{B}} \left\{ \frac{1}{2mn} \|\mathbf{Y} - \mathbf{1}_n \boldsymbol{\beta}_0^\top - \mathbf{X} \mathbf{B}\|_F^2 + \lambda \sum_{j=1}^p \sum_{g \in \mathcal{G}} w_g \|\mathcal{S}_j^g(\mathbf{B})\|_{\ell_{q_{j,g}}} \right\},$$

where  $\mathcal{S}_j^g(\mathbf{B})$  is the a submatrix of  $\mathbf{B}$ ,  $q_{j,g} \in [1, \infty]$ ,  $\lambda$  is a tuning parameter,  $\mathcal{G}$  contains pre-defined groups and all group weights  $w_g$ 's are known or can be pre-estimated. The submatrix  $\mathcal{S}_j^g(\mathbf{B}) = \{\beta_{jk} : j \in M_g, k \in N_g\}$  is associated with specified set of rows  $M_g \subseteq [p]$  and columns  $N_g \subseteq [m]$ . Let  $\mathbf{X} = [\mathbf{X}_1, \dots, \mathbf{X}_S]$  with numbers of features  $p_1, \dots, p_S$ , respectively,  $p = \sum_{s=1}^S p_s$  and  $\mathbf{B} = [\mathbf{B}_1 : \dots : \mathbf{B}_S]$ . The corresponding IPF problem

$$(2.7) \quad \min_{\boldsymbol{\beta}_0, \mathbf{B}} \left\{ \frac{1}{2mn} \|\mathbf{Y} - \mathbf{1}_n \boldsymbol{\beta}_0^\top - \mathbf{X} \mathbf{B}\|_F^2 + \sum_{s=1}^S \sum_{j=1}^{p_s} \sum_{g \in \mathcal{G}} \lambda_s w_g \|\mathcal{S}_j^g(\mathbf{B}_s)\|_{\ell_{q_{j,g}}} \right\}$$

can be transformed into the equivalent original problem

$$\min_{\boldsymbol{\beta}_0, \mathbf{B}^*} \left\{ \frac{1}{2mn} \|\mathbf{Y} - \mathbf{1}_n \boldsymbol{\beta}_0^\top - \mathbf{X}^* \mathbf{B}^*\|_F^2 + \lambda_1 \sum_{j=1}^p \sum_{g \in \mathcal{G}} w_g \|\mathcal{S}_j^g(\mathbf{B}^*)\|_{\ell_{q_{j,g}}} \right\},$$



where  $\mathbf{X}^* = [\mathbf{X}_1, \frac{\lambda_1}{\lambda_2}\mathbf{X}_2, \dots, \frac{\lambda_1}{\lambda_S}\mathbf{X}_S]$ ,  $\mathbf{B}^* = [\mathbf{B}_1: \frac{\lambda_2}{\lambda_1}\mathbf{B}_2: \dots: \frac{\lambda_S}{\lambda_1}\mathbf{B}_S]$  and  $\mathcal{S}_j^g(\mathbf{B}^*) = \{\beta_{jk}^* : j \in M_g, k \in N_g\}$ , if  $\bigcup M_g = [p]$  and  $\bigcup N_g = [m]$ . If  $\bigcup M_g \subsetneq [p]$  and (or)  $\bigcup N_g \subsetneq [m]$ , then the elements  $\{\beta_{jk}^* : j \in [p] \setminus \bigcup M_g, k \in [m] \setminus \bigcup N_g\}$  and the non-penalized features are remained in the Frobenius-norm loss function. The rows in  $M_g$  and the columns in  $N_g$  need not be contiguous, and  $\mathcal{S}_j^g(\mathbf{B}_s)$  can be overlapping.

The Proposition 4 allows different norms for different submatrices in the penalty term. IPF-lasso and IPF-tree-lasso are special cases of (2.7), that is,

- IPF-lasso:  $\mathcal{G} = \{1\}$ ,  $w_g = 1$ ,  $\mathcal{S}_j^g(\mathbf{B}_s) = \mathbf{B}_s$ ,  $\ell_{q_{j,g}} = \ell_1$ ;
- IPF-tree-lasso:  $\mathcal{G} = \{V_{\text{leaf}}, V_{\text{int}}\}$ ,  $\mathcal{S}_j^g(\mathbf{B}_s) = \beta_j^{G_v}$ ,  $\ell_{q_{j,g}} = \ell_2$ .

In (2.6),  $\|\mathcal{S}_j^g(\mathbf{B})\|_{\ell_\infty} = \sup\{|\beta_{jk}| : j \in M_g, k \in N_g\}$  is likely to seek a common subset of a submatrix  $\mathcal{S}_g(\mathbf{B})$ , in which selected features will be relevant to multiple response variables simultaneously (Turlach and others, 2005). The Sparse Group Elastic Net [33] including  $\ell_1$ ,  $\ell_2$  and  $\ell_\infty$  is also a special case of (2.7). Since the penalty term in (2.7) allows the overlaps of submatrices, it can contain more integrated penalty cases. For example, sparse-group lasso [38] with  $\ell_1$  and  $\ell_2$  penalties actually allows the overlaps of coefficient groups (including singletons). Jacob, Obosinski and Vert [20] proposed group lasso allowing overlaps in combination with graphical lasso. Li, Nan and Zhu [27] proposed the multivariate sparse group lasso, where an arbitrary group structure such as overlapping or nested or multilevel hierarchical structure is considered. All these methods can be extended into corresponding IPF-type methods and be solved by Proposition 4. However, (2.7) doesn't include graphical lasso or fused lasso. If there is a non-identity transformation of the submatrix of  $\mathbf{B}$  inside of the norm in the penalty term, the augmented matrix will be complicated.

**2.3. Implementation.** For the implementation, we give an initial decreasing  $\lambda$  sequence, starting at  $\lambda_{\max}$  which shrinks all coefficients to zero [11], for lasso, elastic net, IPF-lasso and sIPF-elastic-net. The multivariate responses  $\mathbf{Y}$  are vectorized to  $\text{vec}(\mathbf{Y})$ . The interval-search algorithm Efficient Parameter Selection vis Global Optimization (EPSGO) is applied to find the optimal  $\alpha$  in elastic net type methods [12, 37], as well as penalty parameters ratios in IPF-type methods. The EPSGO algorithm updates the tuning parameters through learning a Gaussian process model of the loss function surface from the points which have already been visited. Note that parameter tuning for IPF-elastic-net with varying  $\alpha$ 's remains challenging even when using the EPSGO algorithm due to the large number of parameters in a non-convex situation. For IPF-tree-lasso,  $\lambda_1$  is optimized by exploring a

given sequence of values, while the EPSGO algorithm is used to determine the optimal penalty parameters ratios  $\lambda_s/\lambda_1$  ( $s > 1$ ). The IPF-tree-lasso is implemented based on the equivalent tree-lasso problem, which is more efficient than directly adapting the original tree-lasso algorithm to iterate coefficients of different data sources respectively (see Supplementary S3). The tree structure is pre-estimated from the response data by hierarchical agglomerative clustering [14] and only using the nodes with normalized heights larger than a pre-determined threshold  $\rho^*$  to ignore groups with weak correlations between response variables. Optimal penalty parameters are found by minimizing the  $\text{MSE}_{\text{CV}}$  as loss function on the learning data, and independent validation data are used to obtain prediction mean squared errors ( $\text{MSE}_{\text{val}}$ ) to evaluate prediction performance.

### 3. Simulations.

3.1. *Simulation scenario.* We simulate data to demonstrate the prediction performance and variable selection performance of lasso, elastic net, tree-lasso and their corresponding IPF-type methods. We assume multiple responses with  $m = 24$ , two data sources of high-dimensional input features ( $p_1 > n, p_2 > n$ ), and  $n = 100$  samples. The data are simulated according to the linear model

$$(3.1) \quad \mathbf{Y} = [\mathbf{X}_1, \tilde{\mathbf{X}}_2] \begin{bmatrix} \mathbf{B}_1 \\ \mathbf{B}_2 \end{bmatrix} + \mathbf{E}.$$

The high-dimensional feature matrix  $\tilde{\mathbf{X}} = [\mathbf{X}_1, \tilde{\mathbf{X}}_2]$  is generated from a multivariate normal distribution with mean  $\mathbf{0}$  and a nondiagonal  $(p_1 + p_2) \times (p_1 + p_2)$  covariance matrix  $\Sigma$  as Boulesteix and others (2017) suggested  $\tilde{\mathbf{X}} \sim \mathcal{N}(\mathbf{0}, \Sigma \otimes \mathbb{I}_n)$ , where

$$\Sigma = \begin{bmatrix} A_{p_1/b}(\sigma) & \dots & 0 & B_{p_1/b, p_2/b}(\sigma) & \dots & 0 \\ \vdots & \ddots & \vdots & \vdots & \ddots & \vdots \\ 0 & \dots & A_{p_1/b}(\sigma) & 0 & \dots & B_{p_1/b, p_2/b}(\sigma) \\ B_{p_2/b, p_1/b}(\sigma) & \dots & 0 & A_{p_2/b}(\sigma) & \dots & 0 \\ \vdots & \ddots & \vdots & \vdots & \ddots & \vdots \\ 0 & \dots & B_{p_2/b, p_1/b}(\sigma) & 0 & \dots & A_{p_2/b}(\sigma) \end{bmatrix}.$$

Further dichotomizing  $\mathbf{X}_2 = \mathbf{1}_{\{\tilde{\mathbf{X}}_2 > 0\}}$  where  $\mathbf{1}_{\{\cdot\}}$  is an indicator function and let  $\mathbf{X} = [\mathbf{X}_1, \mathbf{X}_2]$ . The second data source is dichotomized to simulate the common situation that one data source represents binary gene mutations. In the covariance matrix  $\Sigma$ , blocks  $A_{p_1/b}(\sigma)$  and  $A_{p_2/b}(\sigma)$  capture the covariances of features among the first and second data source, respectively.

In each data source, there are  $b$  latent groups of size  $(p_1/b) \times (p_1/b)$  and  $(p_2/b) \times (p_2/b)$ , respectively, represented by blocks  $B_{p_1/b, p_2/b}$  and  $B_{p_2/b, p_1/b}$  in which any two features have covariance  $\sigma$ . We set  $\sigma = 0.4$ ,  $b = 10$ , and the variance of each feature is one. Considering that different data sources might have different numbers of features, we simulate two situations,  $(p_1, p_2) = (150, 150)$  and  $(p_1, p_2) = (500, 150)$ . In (3.1), the noise term  $\mathbf{E} = \{\epsilon_{ik}\}$  ( $i \in [n]; k \in [m]$ ), and  $\{\epsilon_{ik}\} \stackrel{iid}{\sim} \mathcal{N}(0, 1)$ .

We assume that multiple responses can be grouped and the group relationships can be addressed by a hierarchical tree structure. In our intended applications, different molecular information may explain different group effects in the drug response variables. In the first simulation scenario, we design two different hierarchical tree effects from the two data sources, as illustrated in Figure 3. The groups in the first 12 response variables are determined by the first data source, and the second data source determines the groups in the second 12 responses. The two hierarchical structures are generated by the two matrices  $\mathbf{B}_1$  and  $\mathbf{B}_2$  illustrated in Figure 3. In a second simulation scenario the two data sources do not determine the drug groups separately, but instead in an overlapping manner. For this we design two very different hierarchical structures with  $\mathbf{B}_1$  and  $\mathbf{B}_2$ , as illustrated in Figure 4. In scenario 3, to test the sensitivity to model misspecification, we set a control case which has no tree-structured  $\mathbf{B}_1$  and  $\mathbf{B}_2$  as shown in Figure 5. The patterns of  $\mathbf{B}_1$  and  $\mathbf{B}_2$  in Figure 5 correspond to the designed "hotspots" in the simulation by Lewin *et al.* [25].

To evaluate the prediction performance of different methods, we calculate  $\text{MSE}_{\text{val}}$  from the simulated validation data  $\mathbf{X}_{\text{val}}$  and  $\mathbf{Y}_{\text{val}}$  which are simulated independently in an identical manner to  $\mathbf{X}$  and  $\mathbf{Y}$ . Additionally, we compare the accuracy of variable selection performance, where we use the terms sensitivity to denote the percentage of nonzero coefficients accurately estimated as nonzeros and specificity to denote the percentage of zero coefficients accurately estimated as zeros. Algorithm 1 below summarizes the simulation study setup.

---

**Algorithm 1:** Simulation study setup to compare the prediction performance of penalized regression

---

**Input :**  $\mathbf{X}$ ,  $\mathbf{Y}$  and validation data  $\mathbf{X}_{\text{val}}$ ,  $\mathbf{Y}_{\text{val}}$  simulated according to simulation scenario 1, 2 or 3 with  $(p_1, p_2) = (150, 150)$  or  $(p_1, p_2) = (500, 150)$ .

**Output:** Prediction performance of the 6 methods, i.e., lasso, elastic net, IPF-lasso, sIPF-elastic-net, tree-lasso, IPF-tree-lasso.

Use hierarchical clustering to obtain a tree  $T$  representing the grouping structure in  $\mathbf{Y}$ .

Split data  $\mathbf{X}$  and  $\mathbf{Y}$  into  $K = 5$  folds, respectively.  $\mathbf{X}_{(-k)}$  and  $\mathbf{Y}_{(-k)}$  exclude the observations of  $k$ th fold, and  $\mathbf{X}_{(k)}$  and  $\mathbf{Y}_{(k)}$  consist of the observations of  $k$ th fold.

**for** method  $M = 1, \dots, 6$  **do**

**for** penalty parameters  $\boldsymbol{\theta}_{M,l} (l = 1, \dots, L_M)$  **do**

**for** fold  $k = 1, \dots, K$  **do**

      i) Estimate  $(\hat{\boldsymbol{\beta}}_{0(-k)}^M, \hat{\mathbf{B}}_{(-k)}^M) \leftarrow \arg \min_{\boldsymbol{\beta}_0, \mathbf{B}} \{ \frac{1}{2mn} \|\mathbf{Y}_{(-k)} - \mathbf{1}_n \boldsymbol{\beta}_0^\top - \mathbf{X}_{(-k)} \mathbf{B}\|_F^2 + \text{pen}_M(\mathbf{B}) \}$  by the  $M$ th method as outlined in Section 2.

      ii) Compute  $\hat{\text{e}}\text{r}_k^M(\boldsymbol{\theta}_{M,l}) \leftarrow \|\mathbf{Y}_{(k)} - \mathbf{1}_n \hat{\boldsymbol{\beta}}_{0(-k)}^{M\top} - \mathbf{X}_{(k)} \hat{\mathbf{B}}_{(-k)}^M\|_F^2$ .

**end**

    Compute cross-validation error

$$\text{MSE}_{\text{CV}}^M(\boldsymbol{\theta}_{M,l}) \leftarrow \frac{1}{K} \sum_{k=1}^K \hat{\text{e}}\text{r}_k^M(\boldsymbol{\theta}_{M,l}).$$

**end**

  i) Obtain optimal penalty parameters

$$\boldsymbol{\theta}_M^{\text{opt}} \leftarrow \arg \min_{\boldsymbol{\theta}_{M,l}} \text{MSE}_{\text{CV}}^M(\boldsymbol{\theta}_{M,l}).$$

  ii) Obtain  $\hat{\boldsymbol{\beta}}_0^M$  and  $\hat{\mathbf{B}}^M$  by fitting  $M$ th model on the full  $\mathbf{X}$  and  $\mathbf{Y}$  using  $\boldsymbol{\theta}_M^{\text{opt}}$ .

  iii) Compute the final prediction error

$$\text{MSE}_{\text{val}}^M(\boldsymbol{\theta}_M^{\text{opt}}) \leftarrow \frac{1}{mn} \|\mathbf{Y}_{\text{val}} - \mathbf{1}_n \hat{\boldsymbol{\beta}}_0^{M\top} - \mathbf{X}_{\text{val}} \hat{\mathbf{B}}^M\|_F^2.$$

**end**

**Result:**  $\text{MSE}_{\text{val}}^M$ ,  $\hat{\boldsymbol{\beta}}_0^M$  and  $\hat{\mathbf{B}}^M$  of all methods,  $M = 1, \dots, 6$ .

---

3.2. *Simulation results and discussion.* We do 50 simulations and show in Figure 6 the prediction performance of all methods in the different scenarios. When the two data sources have the same number of features (i.e.,  $p_1 = p_2 = 150$ ) and similar trees for  $\mathbf{B}_1$  and  $\mathbf{B}_2$  as in scenario 1 (Figure 3),

then lasso, IPF-lasso, elastic net and sIPF-elastic-net have similar prediction performance in terms of  $\text{MSE}_{\text{val}}$  (Figure 6(a)). But tree-lasso and IPF-tree-lasso outperform other methods. However, when the two data sources are more different as in design scenario 2 (Figure 4), IPF-lasso and sIPF-elastic-net are slightly superior to lasso and elastic net in the situation of  $p_1 = p_2 = 150$  (Figure 6 (c)). IPF-tree-lasso further improves the prediction. In the control case, Figure 6 (e) (scenario 3), tree-lasso and IPF-tree-lasso still have better prediction.

When the two data sources have different feature numbers (i.e.,  $p_1 = 500$ ,  $p_2 = 150$ ), IPF-type methods (IPF-lasso, sIPF-elastic-net and IPF-tree-lasso) have lower  $\text{MSE}_{\text{val}}$  than their corresponding non-IPF-type methods (lasso, elastic net and tree-lasso) respectively in all three scenarios (Figure 6 (b), (d) and (f)). When comparing scenario 2 with scenario 1 in the case  $(p_1, p_2) = (500, 150)$ , IPF-type methods improve the prediction more significantly in scenario 2.

Table 1 displays the accuracy of coefficients matrix estimation and variable selection for scenario 1. According to the averaged absolute errors of estimated coefficients,  $\frac{1}{mp} \|\hat{\mathbf{B}} - \mathbf{B}\|_{\ell_1}$ , all methods perform similarly if  $(p_1, p_2) = (150, 150)$  but the IPF-type methods perform slightly better for  $(p_1, p_2) = (500, 150)$ . In both cases,  $(p_1, p_2) = (150, 150)$  and  $(p_1, p_2) = (500, 150)$ , IPF-lasso, sIPF-elastic-net, and IPF-tree-lasso select fewer features and achieve larger specificity than non-IPF-type methods, but they lose sensitivity.

In the simulations, we mainly focus on simulating hierarchically structured drug sensitivity according to the specifically designed coefficient matrices as in Figure 3 (scenario 1) and Figure 4 (scenario 2). In both scenarios 1 and 2, the tree-lasso model improves performance. But even in the case of non-structured  $\mathbf{Y}$  (scenario 3) tree-lasso still outperforms lasso and elastic net in Figure 6(e), because some of the correlation structures among response variables can be captured by a tree structure. For example, the nonzero blocks in  $\mathbf{B}$  in Figure 5 illustrate different response variables that are likely to be similar since these responses can be explained by the same features. Kim and Xing [22] also showed that tree-lasso can take into account such correlations even when the tree structure is not fully realized. Compared to the top three panels of Figure 6, the bottom three panels reflect a greater contribution to prediction performance of IPF-type methods. In all situations, IPF-tree-lasso achieves the best prediction, at least as good as tree-lasso when  $p_1 = p_2 = 150$ , and the IPF-lasso and sIPF-elastic perform quite well when  $(p_1, p_2) = (500, 150)$ . It is because that IPF-tree-lasso does not only consider the correlations among responses, but also distin-

guishes the relative contributions of two data sources with varying penalty parameters  $\lambda_1$  and  $\lambda_2$ .

**4. Real data analysis.** The Genomics of Drug Sensitivity in Cancer (GDSC) database [49] was developed from a large-scale pharmacogenomic study. The drug sensitivity, measured as half-maximal inhibitory concentration ( $IC_{50}$ ), is estimated by fitting a Bayesian sigmoid model to dose-response curves obtained for a range of drug concentrations corresponding to the 72 hours' effect of drug treatment on cell viability, see Garnett *et al.* [13] for the modelling details. We use the data from their archived files in <ftp://ftp.sanger.ac.uk/pub4/cancerrxgene/releases/release-5.0/>, where there are 97 cancer drugs tested for 498 cell lines with complete availability of  $IC_{50}$  after excluding one cell line with an extremely small estimate for  $IC_{50} = 1.43 \times 10^{-16} \mu M$ . These cell lines are from 13 cancer tissue types. For each cell line, the following genomic data are available as baseline measurements: genome-wide measurement of mRNA expression, copy numbers and DNA single point and other mutations. We preselected 2602 gene expression features with the largest variances over cell lines, which in total explain 50% of the variation. Referring to the Cancer Gene Census (<https://cancer.sanger.ac.uk/census>), copy number variations for 426 genes and mutations in 68 genes are causally implicated in cancer.

We randomly select 80% cell lines of each cancer tissue type for training data and the other 20% as validation data. A multivariate regression model is fitted to the 80% training data:

$$(4.1) \quad \mathbf{Y} = \mathbf{1}_n \boldsymbol{\beta}_0^\top + \mathbf{X}_0 \mathbf{B}_0 + \mathbf{X} \mathbf{B} + \mathbf{E},$$

where  $\mathbf{Y}$  is the  $\log_e IC_{50}$  to reduce the skewness of  $IC_{50}$ ,  $\boldsymbol{\beta}_0$  is the intercept vector,  $\mathbf{X}_0$  represents the cancer tissue types by dummy variables, and  $\mathbf{X} = [\mathbf{X}_1, \mathbf{X}_2, \mathbf{X}_3]$  consists of the  $\log_e$ -transformed gene expression variables ( $\mathbf{X}_1$ ), the copy number variables ( $\mathbf{X}_2$ ) and mutation (0/1) variables ( $\mathbf{X}_3$ ). Let  $\mathbf{B} = [\mathbf{B}_1 : \mathbf{B}_2 : \mathbf{B}_3]$  correspond to the coefficient matrices of the three data sources. Since tissue types are known to have large effects on drug sensitivity and  $\mathbf{X}_0$  is low-dimensional, we do not penalize the coefficients  $\mathbf{B}_0$  of cancer tissue types when fitting the model (4.1). Supplementary S5 outlines the estimation of non-penalized coefficients in the tree-lasso model. The 20% validation data are used to evaluate prediction performance by  $MSE_{\text{val}}$ . The implementation procedure of (4.1) by all methods is the same as shown in the simulation Algorithm 1. Additionally,  $R_{\text{val}}^2$  is computed as

$$R_{\text{val}}^2 \equiv 1 - \frac{SSE_{\text{val}}}{SST_{\text{val}}} = 1 - \frac{\|\mathbf{Y}_{\text{val}} - \mathbf{1}_n \hat{\boldsymbol{\beta}}_0^\top - \mathbf{X}_{\text{val}} \hat{\mathbf{B}}\|_F^2}{\|\mathbf{Y}_{\text{val}} - \mathbf{1}_n \bar{\mathbf{Y}}_{\text{val}}\|_F^2},$$

where  $\mathbf{X}_{\text{val}}$  and  $\mathbf{Y}_{\text{val}}$  are the 20% validation data,  $\bar{\mathbf{Y}}_{\text{val}}$  is a column vector with averaged  $\log_e \text{IC}_{50}$  of each drug over the validation data samples. For comparison we also fit two low-dimensional linear regression models: (1) the "NULL" model which only includes an intercept vector, and (2) the "OLS" model which includes the intercept vector and dummies  $\mathbf{X}_0$  of the cancer tissue types.

To eliminate the uncertainty of splitting the data randomly into training|validation sets, Table 2 reports the averaged results of 10 different random splits of the GDSC data. When only using the 13 tissue categories as predictors ("OLS" model), the prediction performance is very poor,  $\text{MSE}_{\text{val}}=3.199$  and  $\bar{R}_{\text{val}}^2 = 3.64\%$  averaged over the 10 repetitions. However, the genomic information improves the prediction in the lasso and elastic net models as shown in Table 2. By taking into account the hierarchical group relationship of 97 drugs (tree-lasso and IPF-tree-lasso) and the heterogeneity of different data sources (IPF-type methods), performance can be improved further. IPF-tree-lasso performs best, with prediction  $\text{MSE}_{\text{val}}=3.025$  and  $\bar{R}_{\text{val}}^2 = 8.89\%$ . Nevertheless, all methods explain only a limited percentage of variation in the drug sensitivity data when averaging across all drugs. When looking at the individual explained variation  $\bar{R}_{\text{val}}^2$  and  $\text{MSE}_{\text{val}}$ , the results differ widely between drugs. For example, the molecular information via the IPF-tree-lasso model can explain 44.75% variation of Nutlin-3 $\alpha$  drug sensitivity (Figure S2 of Supplementary S6). More prediction results with discussion for individual drugs and tissues can be found in Supplementary S6.

In Table 2,  $VS^* = \sum_{j=1}^p \sum_{k=1}^m \left\{ \left( \sum_{r=1}^{10} \mathbf{1}_{\{\hat{\beta}_{jk}^{(r)} \neq 0\}} \right) \geq 2 \right\}$  indicates the features selected at least twice over the 10 repetitions. We note that lasso, elastic net and IPF-lasso perform very sparse variable selection with fewer than 860 out of  $p \times m = 300312$  (0.29%) nonzero features estimated more than once over 10 repetitions. Although sIPF-elastic-net has better average prediction performance, it results in an almost full dense coefficients matrix with averaged  $\alpha = 0.39$ , but elastic net with averaged  $\alpha = 0.77$ . Tree-lasso obtains a much larger number of nonzero coefficients for copy number features than IPF-tree-lasso, but only one associated mutation variable: TP53 for drug Nutlin-3 $\alpha$ . In contrast, IPF-tree-lasso selects 537 associated mutated gene features, in particular, targeted mutant B-Raf for drugs PLX4720 and SB590885, mutant EGFR/ErbB for BIBW2992 (Afatinib), and the chromosomal rearrangement Bcr-Abl for drugs Nilotinib and AP-24534. All these mutations are in target genes of the corresponding drugs and were thus expected to be important for the prediction of drug sensitivity.

**5. Conclusion.** In this study, we used multi-omics data to predict sensitivity of cancer cell lines to multiple drugs jointly. The penalized regression should take into account the heterogeneity in the multi-omics data as well as (hierarchical) relationships between drugs. We extended the tree-lasso to IPF-tree-lasso, which can achieve the two purposes simultaneously. Through weighting the data by the penalty parameters, Proposition 3 makes the implementation of IPF-tree-lasso feasible. In addition, based on IPF-lasso [5], we formulated the IPF-elastic-net, which is an option to tune the varying penalty parameters  $\lambda_s$  and  $\alpha_s$  ( $s \in [S]$ ) in (2.3), thus allowing differing degrees of sparsity in the different data sources. If one has prior knowledge on the sparsity of the different data sources, IPF-elastic-net can specify some data sources as lasso for instance, i.e., those  $\alpha$ 's as 1. Proposition 4 provides the transformation from a large class of general IPF-type penalized problems into the equivalent original penalized problems. Furthermore, we demonstrated how the interval-search algorithm EPSGO [12] can be used to optimize multiple penalty parameters efficiently.

To capture the heterogeneity of different features, Bergersen, Gland and Lyng [4] proposed weighted lasso to use external information (i.e., copy numbers) to generate penalty weights. Van de Wiel *et al.* [44] developed "GRridge" regression to use related co-data (annotation or external  $p$  values) to derive group-specific penalties by empirical Bayes estimation; only one global penalty parameter needs to be optimized by e.g. cross-validation. These methods use other data as auxiliary data to determine (group) weights in the penalty term. However, in IPF-type methods all data information contributes to the outcomes directly. Dondelinger and Mukherjee [10] proposed joint lasso to penalize subgroup-specific (i.e., cancer tissue) coefficients differently with an additional fusion penalty term, but they used the same penalty for high-dimensional features. Klau *et al.* [23] presented priority-Lasso to construct blocks of multi-omics data sources and regress on each data source sequentially. Wu *et al.* [48] selectively reviewed multi-level omics data integration methods, but focused on univariate and survival outcomes.

In the GDSC data analysis, the low averaged  $\bar{R}_{\text{val}}^2$  implies the limitation to use genomic information to predict drug sensitivity. Wang *et al.* [45] and Ali *et al.* [1] showed proteomes of human cancer cell lines are more representative of primary tumors than genomic profiles alone to predict drug sensitivity. Chambliss and Chan [6] recommended to integrate pharmacoproteomic and pharmacogenomics profiles to identify the right therapeutic regimen. Also, the heterogeneity between cell lines even within one cancer tissue type might be large [2, 30].

One disadvantage of IPF-type methods is that they cannot address known



associations between features in the different data sources, e.g., between gene expression and mutation status of the same gene. However, the sIPF-elastic-net employs a common  $\alpha$  for all data sources, which is likely to select the strongly correlated features over all data sources together if  $\alpha$  is small (Theorem 1). As for IPF-tree-lasso, specifying similar weights for coefficients of associated internal nodes in (2.5) across different data sources may select correlated features over multiple data sources. Furthermore, using biological pathways of genes related to the cancer may improve the biological interpretation and prediction of drug sensitivity as well. Lee *et al.* [24] and Li and Li [26] proposed pathway-based approaches to identify biologically relevant pathways related to interesting phenotype. The tree-lasso or IPF-tree-lasso can also be extended to include the pathway-group structure over features in the penalty term besides the hierarchical structure over response variables.

#### ACKNOWLEDGEMENTS

The first author is supported by the Faculty of Medicine, University of Oslo, Norway. This work is associated with the Norges Forskningsråd project BIG INSIGHT: 237718. The authors thank Professor Arnoldo Frigessi for discussions. *Conflict of Interest*: None declared.

#### SUPPLEMENTARY MATERIAL

Software in the form of R package `IPFStructPenalty`, together with a sample input data set and complete documentation is available on <https://github.com/zhizui/IPFStructPenalty>. Other supplementary materials including proofs, extra algorithms and results with discussion are available online.

#### REFERENCES

- [1] ALI, M., KHAN, S.A., WENNERBERG, K. AND AITTOKALLIO, T.(2018). Global proteomics profiling improves drug sensitivity prediction: results from a multi-omics, pan-cancer modeling approach. *Bioinformatics* **34**, 1353-1362.
- [2] ARUL, M., ROSLANI, A.C. AND CHEAH, S.H.(2017). Heterogeneity in cancer cells: variation in drug response in different primary and secondary colorectal cancer cell lines in vitro. *In Vitro Cellular & Developmental Biology - Animal* **53**, 435-447.
- [3] BARRETINA, J., CAPONIGRO, G., STRANSKY, N., VENKATESAN, K., MARGOLIN, A.A., KIM, S., WILSON, C.J., LEHAR, J., KRYUKOV, G.V., SONKIN, D. *et al.*(2012). The Cancer Cell Line Encyclopedia enables predictive modelling of anticancer drug sensitivity. *Nature* **483**, 603-607.
- [4] BERGERSEN, L.C., GLAD, I.K. AND LYNG, H.(2011). Weighted lasso with data integration. *Statistical Applications in Genetics and Molecular Biology* **10**, 1-29.
- [5] BOULESTEIX, A.L., DE BIN, R., JIANG, X. AND FUCHS, M.(2017). IPF-LASSO: integrative L1- penalized regression with penalty factors for prediction based on multi-omics data. *Computational and Mathematical Methods in Medicine* 7691937.

- [6] CHAMBLISS, A.B. AND CHAN, D.W.(2016). Precision medicine: from pharmacogenomics to pharmacoproteomics. *Clinical Proteomics* 13-25.
- [7] CHEN, X., LIN, Q., KIM, S., CARBONELL, J. AND XING, E.(2012). Smoothing proximal gradient method for general structured sparse regression. *The Annals of Applied Statistics* **6**, 719-752.
- [8] CHIU, S.J., UENO N.T. AND LEE, R.J.(2004). Tumor-targeted gene delivery via anti-HER2 antibody (trastuzumab, Herceptin) conjugated polyethylenimine. *Journal of Controlled Release* **97**, 357-369
- [9] DAEMEN, A., GRIFFITH, O.L., HEISER, L.M., WANG, N.J., ENACHE, O.M., SANBORN, Z., PEPIN, F., DURINCK, S., KORKOLA, J.E., GRIFFITH, M. *et al.* (2013). Modeling precision treatment of breast cancer. *Genome Biology* **14**, R110.
- [10] DONDELINGER, F. AND MUKHERJEE, S. (2018). The joint lasso: high-dimensional regression for group structured data. *Biostatistics* kxy035.
- [11] FRIEDMAN, J., HASTIE, T. AND TIBSHIRANI, R.(2010). Regularization Paths for Generalized Linear methods via Coordinate Descent. *Journal of Statistical Software* **33**, 1-22.
- [12] FROHLICH, H. AND ZELL, A.(2005). Efficient Parameter Selection for Support Vector Machines in Classification and Regression via Model-Based Global Optimization. Proceedings of the International Joint Conference of Neural Networks *pp* 1431-1438.
- [13] GARNETT, M., EDELMAN, E., HEIDORN, S., GREENMAN, C.D., DASTUR, A., LAU, K.W., GRENINGER, P., THOMPSON, I.R., LUO, X., SOARES, J. *et al.*(2012). Systematic identification of genomic markers of drug sensitivity in cancer cells. *Nature* **483**, 570-575.
- [14] GOLUB, T., SLONIM, D., TAMAYO, P., HUARD, C., GAASENBEEK, M., MESIROV, J.P., COLLIER, H., LOH, M.L., DOWNING, J.R., CALIGIURI, M.A., BLOOMFIELD, C.D. AND LANDER, E.S. (1999). Molecular classification of cancer: class discovery and class prediction by gene expression monitoring. *Science* **286**, 531-537.
- [15] GRESHOCK, J., BACHMAN, K.E., DEGENHARDT, Y.Y., JING, J., WEN, Y.H., EASTMAN, S., MCNEIL, E., MOY, C., WEGRZYN, R., AUGER, K., HARDWICKE, M.A. AND WOOSTER, R. (1999). Molecular target class is predictive of in vitro response profile. *Cancer Research* **70**, 3677-3686.
- [16] HANAHAN, D. AND WEINBER, R.A. (2011). Hallmarks of cancer: the next generation. *Cell* **144**, 646-674.
- [17] HASIN, Y., SELDIN, M. AND LUSIS, A. (2017). Multi-omics approaches to disease. *Genome Biology* **18**, 83.
- [18] HAVERTY, P.M., LIN, E., TAN, J., YU, Y., LAM, B., LIANOGLU, S., NEVE, R.M., MARTIN, S., SETTLEMAN, J., YAUCH, R.L. AND BOURGON, R. (2016). Reproducible pharmacogenomic profiling of cancer cell line panels. *Nature* **533**, 333-337.
- [19] IVERSEN, C., LARSON, G., LAI, C., YEH, L.T., DADSON, C., WEINGARTEN, P., APPLEBY, T., VO, T., MADERNA, A., VERNIER, J.M., HAMATAKE, R., MINER, J.N. AND QUART, B. (2009). RDEA119/BAY 869766: a potent, selective, allosteric inhibitor of MEK1/2 for the treatment of cancer. *Cancer Research* **69**, 6839-6847.
- [20] JACOB, L., OBOZINSKI, G. AND VERT, J.(2009). Group Lasso with Overlap and Graph Lasso. *Proceedings of the 26th Annual International Conference on Machine Learning* **pp**, 433-440.
- [21] JONES, D., SCHONLAU, M. AND WELCH, W.(1998). Efficient Global Optimization of Expensive Black-Box Functions. *Journal of Global Optimization* **12**, 455-492.
- [22] KIM, S. AND XING, E.(2012). Tree-guide group lasso for multi-response regression with structured sparsity, with an application to eQTL mapping. *The Annals of Applied Statistics* **6**, 1095-1117.

- [23] KLAU, S., JURINOVIC, V., HORNUNG, R., HEROLD, T. AND BOULESTEIX, A.L.(2018). Priority-Lasso: a simple hierarchical approach to the prediction of clinical outcome using multi-omics data. *BMC Bioinformatics* **19**, 322.
- [24] LEE, S., CHOI, S., KIM, Y.J., KIM, B.J., T2D-GENES CONSORTIUM, HWANG, H. AND PARK, T.(2016). Pathway-based approach using hierarchical components of collapsed rare variants. *Bioinformatics* **32** 586-594.
- [25] LEWIN, A., SAADI, H., PETERS, J., MORENO-MORAL, A., LEE, J.C., SMITH, K.G., PETRETTO, E., BOTTOLO, L. AND RICHARDSON, S.(2016). MT-HESS: an efficient Bayesian approach for simultaneous association detection in OMICS datasets, with application to eQTL mapping in multiple tissues. *Bioinformatics* **32**, 523-532.
- [26] LI, C. AND LI, H.(2008). Network-constrained regularization and variable selection for analysis of genomic data. *Bioinformatics* **24**, 1175-1182.
- [27] LI, Y., NAN, B. AND ZHU, J.(2015). Multivariate Sparse Group Lasso for the Multivariate Multiple Linear Regression with an Arbitrary Group Structure. *Biometrics* **71**, 354-363.
- [28] LIU, D., YANG, Z., WANG, T., YANG, Z., CHEN, H., HU, Y., HU, C., GUO, L., DENG, Q., LIU, Y., YU, M., SHI, M., DU, N. AND GUO, N.(2016).  $\beta$ 2-AR signaling controls trastuzumab resistance-dependent pathway. *Oncogene* **35**, 47-58.
- [29] LUKE, J. AND HODI, F.S.(2012). Vemurafenib and BRAF Inhibition: A New Class of Treatment for Metastatic Melanoma. *Clinical Cancer Research* **18**, 9-14.
- [30] MEACHAM, C.E. AND MORRISON, S.J.(2013). Tumor heterogeneity and cancer cell plasticity. *Nature* **501**, 328-337.
- [31] MIDDLETON, M.R., FRIEDLANDER, P., HAMID, O., DAUD, A., PLUMMER, R., FALOTICO, N., CHYLA, B., JIANG, F., MCKEEGAN, E., MOSTAFA, N.M. *et al.*(2015). Randomized phase II study evaluating veliparib (ABT-888) with temozolomide in patients with metastatic melanoma. *Annals of Oncology* **26**, 2173-2179.
- [32] NEWMAN, B., LIU, Y., LEE, H.F., SUN, D. AND WANG, Y.(2012). HSP90 inhibitor 17-AAG selectively eradicates lymphoma stem cells. *Cell Reports* **72**, 4551-4561.
- [33] SAMAROV, D., ALLEN, D., HWANG, J., LEE, Y.J. AND LITORJA, M.(2017). A coordinate-descent-based approach to solving the sparse group elastic net. *Technometrics* **59**, 437-445.
- [34] SANDRI, S., FAIAO-FLORES, F., TIAGO, M., PENNACCHI, P.C., MASSARO, R.R., ALVES-FERNANDES, D.K., BERARDINELLI, G.N., EVANGELISTA, A.F., DE LIMA VAZQUEZ, V., REIS, R.M. AND MARIA-ENGLER, S.S.(2016). Vemurafenib resistance increases melanoma invasiveness and modulates the tumor microenvironment by MMP-2 upregulation. *Pharmacological Research* **111**, 523-533.
- [35] SEBOLT-LEOPOLD, J.S.(2000). Development of anticancer drugs targeting the MAP kinase pathway. *Oncogene* **19**, 6594-6599.
- [36] SHI, Y., MA, I.T., PATEL, R.H., SHANG, X., CHEN, Z., ZHAO, Y., CHENG, J., FAN, Y., ROJAS, Y., BARBIERI, E. *et al.*(2015). NSC-87877 inhibits DUSP26 function in neuroblastoma resulting in p53-mediated apoptosis. *Cell Death & Disease* **6**, e1841.
- [37] SILL, M., HIELSCHER, T., BECKER, N. AND ZUCKNICK, M.(2014). c060: Extended Inference with Lasso and elastic net Regularized Cox and Generalized Linear methods. *Journal of Statistical Software* **62**, 1-22.
- [38] SIMON, N., FRIEDMAN, J., HASTIE, T. AND TIBSHIRANI, R.(2012). A sparse-group Lasso. *Journal of Computational and Graphical Statistics* **22**, 231-245.
- [39] SIMON, N., FRIEDMAN, J. AND HASTIE, T.(2013). A blockwise descent algorithm for group-penalized multiresponse and multinomial regression. *arXiv* 1311.6529.
- [40] SONTAKE, V., WANG, Y., KASAM, R.K., SINNER, D., REDDY, G.B., NAREN, A.P., MCCORMACK, F.X., WHITE, E.S., JEGGA, A.G. AND MADALA, S.K.(2017). Hsp90

- regulation of fibroblast activation in pulmonary fibrosis. *JCI Insight* **2**, e91454.
- [41] TANAKA, R., TOMOSUGI, M., SAKAI, T. AND SOWA, Y.(2006). MEK Inhibitor Suppresses Expression of the miR-17-92 Cluster with G1-Phase Arrest in HT-29 Human Colon Cancer Cells and MIA PaCa-2 Pancreatic Cancer Cells. *Anticancer Research* **36**, 4537-4543.
- [42] TIBSHIRANI, R.(1996). Regression shrinkage and selection via the lasso. *Journal of the Royal Statistical Society B* **58**, 267-288.
- [43] TURLACH, B., VENABLES, W. AND WRIGHT, S.(2005). Simultaneous Variable Selection. *Technometrics* **47**, 349-363.
- [44] VAN DE WIEL, M.A., LIEN, T.G., VERLAAT, W., VAN WIERINGEN, W.N., WILTING, S.M.(2016). Better prediction by use of co-data: adaptive group-regularized ridge regression. *Statistics in Medicine* **35**, 368-381.
- [45] WANG, J., MOURADOV, D., WANG, X., JORISSEN, R.N., CHAMBERS, M.C., ZIMMERMAN, L.J., VASAIKAR, S., LOVE, C.G., LI, S., LOWES, K. *et al.*(2017). Colorectal Cancer Cell Line Proteomes Are Representative of Primary Tumors and Predict Drug Sensitivity. *Gastroenterology* **153**, 1082-1095.
- [46] WEBER, H., VALBUENA, J.R., BARBHUIYA, M.A., STEIN, S., KUNKEL, H., GARCIA, P., BIZAMA, C., RIQUELME, I., ESPINOZA, J.A. AND KURTZ, S.D.(2017). Small molecule inhibitor screening identified HSP90 inhibitor 17-AAG as potential therapeutic agent for gallbladder cancer. *Oncotarget* **8**, 26169-16184.
- [47] WEISS, B., PLOTKIN, S., WIDEMANN, B., TONSGARD, J., BLAKELEY, J., ALLEN, J., SCHORRY, E., KORF, B., ROSSER, T., GOLDMAN, S. *et al.*(2018). NFM-06. NF106: Phase 2 trial of the MEK inhibitor PD-0325901 in adolescents and adults with NF1-related plexiform neurofibromas: an NF clinical trials consortium study. *Neuro-Oncology* **20**, i143.
- [48] WU, C., ZHOU, F., REN, J., LI, X., JIANG, Y. AND MA, S.(2017). A Selective review of multi-level omics data integration using variable selection. *High-Throughput* **8**, 4.
- [49] YANG, W., SOARES, J., GRENINGER, P., EDELMAN, E.J., LIGHTFOOT, H., FORBES, S., BINDAL, N., BEARE, D., SMITH, J.A., THOMPSON, I.R. *et al.*(2013). Genomics of Drug Sensitivity in Cancer (GDSC): a resource for therapeutic biomarker discovery in cancer cells. *Nucleic Acids Reserch* **41**, D955-961.
- [50] ZOU, H. AND HASTIE, T.(2005). Regularization and variable selection via the elastic net. *Journal of Royal Statistics Society, Series B* **67**, 301-320.

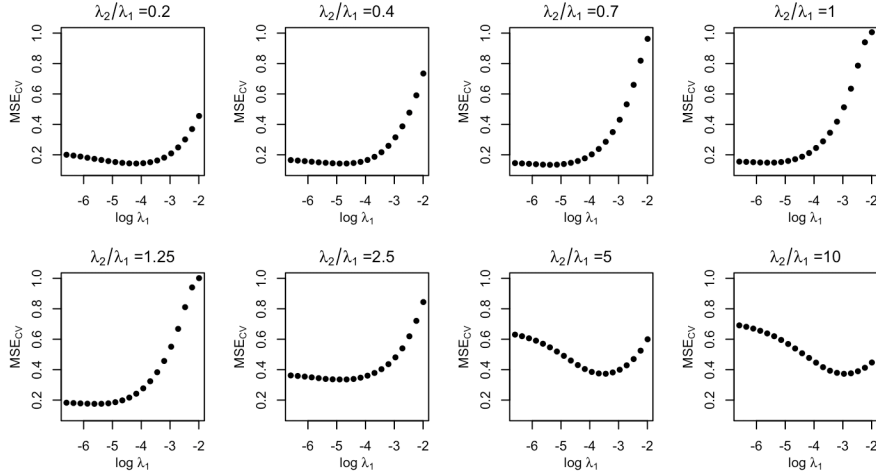


Fig 1: Prediction performance of IPF-lasso for  $(n, m, p_1, p_2) = (100, 24, 500, 150)$  with different penalty parameter ratios  $\lambda_2/\lambda_1$ . It is exactly lasso when  $\lambda_2/\lambda_1 = 1$ . The details of the simulated data are as scenario 2 in Section 3.1.

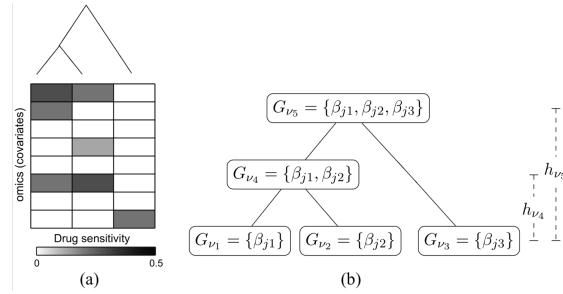


Fig 2: An illustration of a tree lasso with three drugs (figure courtesy of Kim and Xing, 2012). (a): The sparse coefficients matrix is shown with white blocks for zeros and grey blocks for nonzero values. The hierarchical clustering tree above represents the correlation structure in drugs. The first two drugs corresponding to the first two columns are highly correlated and have two common influence covariates (1st and 6th rows). (b): Groups of coefficients associated with each node of the tree in panel (a) in the tree-lasso penalty.  $\beta_{jk} (j \in [8], k \in [3])$  denotes the coefficient of the  $k$ th drug's  $j$ th variable.

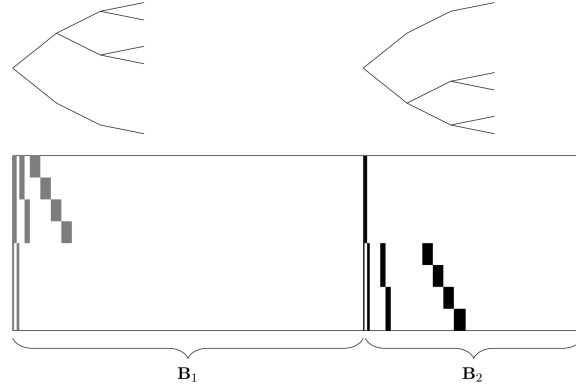


Fig 3: Simulation scenario 1: structured  $\mathbf{B}_1$  and  $\mathbf{B}_2$  corresponding to hierarchical trees to generate hierarchically structured  $\mathbf{Y}$ . Black blocks indicate coefficient values of 0.6, grey blocks 0.2 and white blocks 0. There are 432 nonzero coefficients in total. The two dendrograms on top of  $\mathbf{B}$  show the hierarchical relationships of multivariate responses generated by  $\mathbf{B}_1$  and  $\mathbf{B}_2$ , respectively.

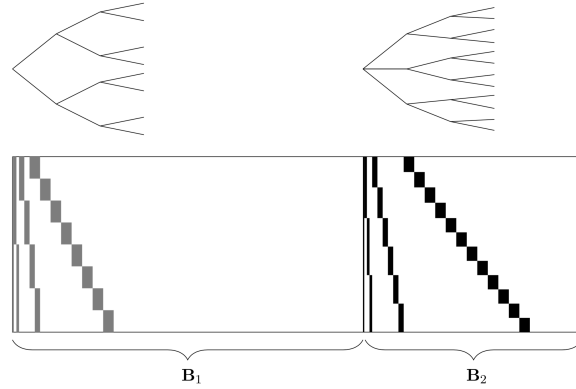


Fig 4: Simulation scenario 2: structured  $\mathbf{B}_1$  and  $\mathbf{B}_2$  corresponding to hierarchical trees to generate hierarchically structured  $\mathbf{Y}$ . Black blocks indicate coefficient values of 0.6, grey blocks 0.2 and white blocks 0. There are 720 nonzero coefficients in total. The two dendrograms on top of  $\mathbf{B}$  show the hierarchical relationships of multivariate responses generated by  $\mathbf{B}_1$  and  $\mathbf{B}_2$ , respectively.

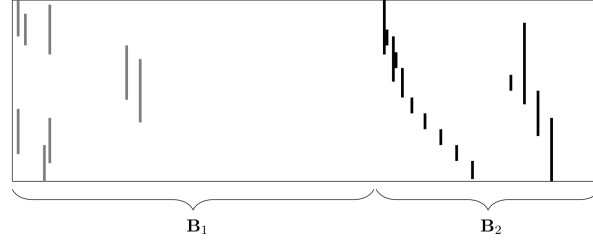


Fig 5: Simulation scenario 3: non-structured  $\mathbf{B}_1$ ,  $\mathbf{B}_2$  to generate non-structured  $\mathbf{Y}$ . Black blocks indicate coefficient values of 0.6, grey blocks 0.2 and white blocks 0. There are 216 nonzero coefficients in total.

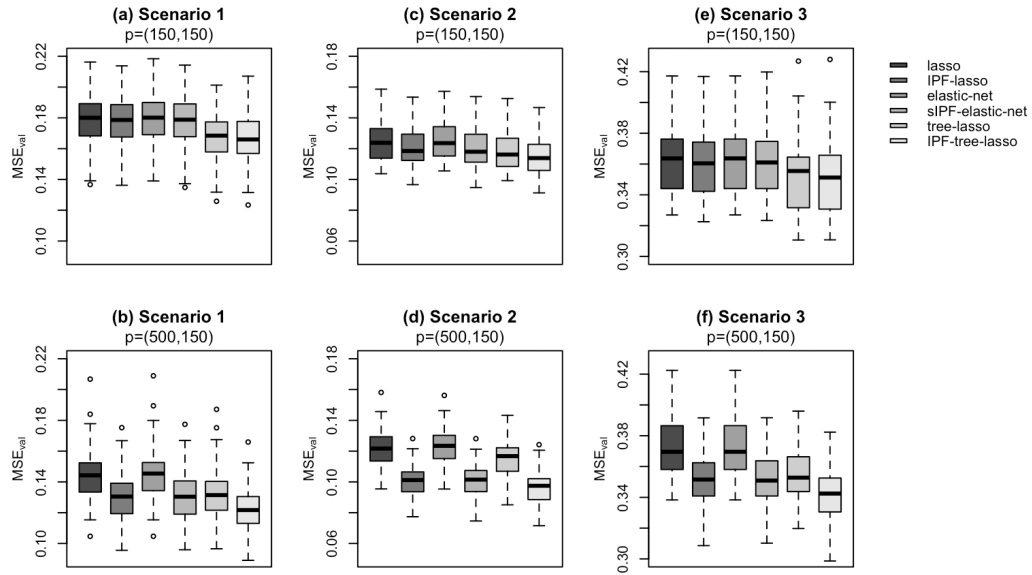


Fig 6: Comparison of  $\text{MSE}_{\text{val}}$  between different approaches in the three simulation scenarios with 50 simulations. The three panels of top are based on the same feature number of  $\mathbf{X}_1$  and  $\mathbf{X}_2$ ,  $p_1 = p_2 = 150$ . The three panels of bottom are based on  $p_1 = 500$  features of  $\mathbf{X}_1$  and  $p_2 = 150$  features of  $\mathbf{X}_2$ .

TABLE 1  
*Accuracy of coefficients recovery by simulated hierarchical structured  $\mathbf{Y}$  as scenario 1*

Model	$\frac{1}{mp} \ \hat{\mathbf{B}} - \mathbf{B}\ _{\ell_1}$	sensitivity	specificity	$VS$
	$p_1 = 150, p_2 = 150$			
Lasso	0.021	0.835	0.904	1008
IPF-lasso	0.021	0.789	0.912	940
Elastic-net	0.022	0.850	0.891	1103
sIPF-elastic-net	0.022	0.806	0.901	1016
Tree-lasso	0.022	0.926	0.671	2627
IPF-tree-lasso	0.022	0.917	0.680	2564
$p_1 = 500, p_2 = 150$				
Lasso	0.022	0.823	0.943	1219
IPF-lasso	0.021	0.758	0.959	950
Elastic-net	0.023	0.838	0.936	1329
sIPF-elastic-net	0.021	0.769	0.955	1011
Tree-lasso	0.024	0.918	0.755	4121
IPF-tree-lasso	0.022	0.903	0.790	3569

All results are the average of 50 simulations. Sensitivity denotes the percentage of nonzero coefficients estimated as nonzeros and specificity to denote the percentage of zero coefficients estimated as zeros. The variable selection index  $VS = \sum_{j=1}^p \sum_{k=1}^m \mathbf{1}_{\{\hat{\beta}_{jk}^{(r)} \neq 0\}}$  indicates the number of selected features.



TABLE 2  
*Prediction and the numbers of selected features in the GDSC data analysis*

Method	NULL	Lasso	elastic net	Tree-lasso
$VS^*$	-	302+1+92	315+1+93	21928+8149+1
$MSE_{CV}$ (s.e.)	3.360(0.027)	3.200 (0.040)	3.198 (0.039)	3.138 (0.040)
$MSE_{val}$ (s.e.)	3.368 (0.107)	3.151 (0.077)	3.149 (0.077)	3.069 (0.079)
$\bar{R}_{val}^2/\%$ (s.e.)	-1.42 (0.84)	5.10 (1.24)	5.17 (1.36)	7.56 (1.87)
	OLS	IPF-lasso	sIPF-elastic-net	IPF-tree-lasso
$VS^*$	-	774+11+74	252394+41322+6596	30567+515+452
$MSE_{CV}$ (s.e.)	3.013 (0.016)	3.182 (0.037)	3.179 (0.036)	3.068 (0.035)
$MSE_{val}$ (s.e.)	3.199 (0.074)	3.134 (0.078)	3.130 (0.076)	3.025 (0.074)
$\bar{R}_{val}^2/\%$ (s.e.)	3.64 (1.63)	5.62 (1.41)	5.72 (1.45)	8.89 (1.75)

The variable selection index  $VS^* = \sum_{j=1}^p \sum_{k=1}^m \left\{ \left( \sum_{r=1}^{10} \mathbf{1}_{\{\hat{\beta}_{jk}^{(r)} \neq 0\}} \right) \geq 2 \right\}$  indicates the features selected at least twice over the 10 repetitions. The NULL model is  $\mathbf{Y} = \mathbf{1}_n \boldsymbol{\beta}_0^\top + \mathbf{E}$ . The OLS model only includes the 13 cancer tissue types information as predictors, i.e.,  $\mathbf{Y} = \mathbf{1}_n \boldsymbol{\beta}_0^\top + \mathbf{X}_0 \mathbf{B}_0 + \mathbf{E}$  where  $(\hat{\boldsymbol{\beta}}_0, \hat{\mathbf{B}}_0)$  are OLS estimates. The number of estimated nonzero coefficients,  $\#\{\hat{\beta}_{jk} \neq 0 : j \in [p], k \in [m]\}$ , corresponds to the mRNA expression, copy numbers and mutation, which are selected at least twice in the 10 repetitions over all drugs.  $MSE_{cv}$  is the average of the mean squared error of 5-fold cross-validation based on the 80% training cell lines, and  $MSE_{val}$  is the average of the 10 repetitions of predicted mean squared error based on the 20% testing cell lines. The range of  $\bar{R}_{val}^2$  is  $(-\infty, 1]$ . The s.e. is the standard derivation over the 10 repetitions.